Rotationally Resolved Infrared Laser Spectroscopy of $(H_2)_n$-HF and $(D_2)_n$-HF ($n = 2-6$) in Helium Nanodroplets

David T. Moore[†] **and Roger E. Miller***

Department of Chemistry, University of North Carolina, Chapel Hill, North Carolina 27599

Received: August 29, 2003; In Final Form: November 21, 2003

Rotationally resolved vibrational spectra are reported for a total of 15 hydrogen-HF clusters formed in helium nanodroplets, each with a different size (up to 6 hydrogens), or isotopic (H_2/D_2) or ortho/para composition. All of these spectra correspond to H−F stretch excitation and are well represented as symmetric or near symmetric prolate tops; fitted rotational constants are presented. Symmetry breaking in the mixed ortho/para complexes gives rise to both parallel and perpendicular transitions in the $(H_2)_n$-HF complexes, whereas only parallel transitions are observed in the spectra of the mixed ortho/para $(D_2)_n$-HF complexes. This difference, as well as the general trends in the rotational constants, can be understood in terms of the relative zero-point energies of the H_2 and D_2 complexes. Evidence of significant delocalization of the solvating hydrogen molecules is presented for larger pure para hydrogen clusters ($n = 4-6$).

Introduction

Hydrogen clusters are of considerable current interest, in part owing to their highly quantum nature.[1−6] The low mass of and weak interactions between hydrogen molecules make them ideal for the study of quantum solvation. Indeed, recent infrared spectroscopic studies of size-dependent trends in doped hydrogen clusters have revealed some fascinating quantum mechanical phenomena. For example, Grebenev et al.[1] studied carbonyl sulfide-para hydrogen (OCS-$(pH_2)_n$) clusters formed within helium nanodroplets at both 0.37 and 0.18 K. They attributed changes in the spectrum with cluster size and temperature to the activation of long-range quantum exchange in the hydrogen solvent. Although superfluidity had been previously predicted in finite para-H_2 clusters,[6] and a subsequent study on $(pH_2)_{17}$-OCS by Kwon and Whaley further supports the existence of a microscopic superfluid state,[4] it is still unclear if the experimental results are indicative of this behavior. Indeed, the effects of the dopant molecule on the superfluid properties are still not well understood and are deserving of further study.

In a recent study of HCN-$(HD)_n$ complexes, we observed dramatic size-dependent solvation effects on the rotational dynamics of the HCN molecule.[2] Specifically, for complexes with $n < 12$ and $n > 13$, "normal" rovibrational spectra were observed, showing P, Q, and R branches indicative of rotation of the entire complex as a unit. In contrast, the HCN molecule was found to undergo nearly free rotation within the solvent cage of the hydrogen for $n = 12$. The evidence for this came from the fact that the associated spectrum consisted of a single R(0) transition, shifted ~ 3 cm^{-1} to the blue of the vibrational origin of the complex,[2] the latter being measured using pendular state spectroscopy.[2]

The magnitude of the solvent cage anisotropy needed to quench the free rotation of a solute molecule depends directly the rotational constant of the latter. The smaller the associated rotational constants, the weaker the anisotropy needed to lock the solute rotation to the solvent cage. In a recent study of these effects, we reported vibrational spectra for hydrogen fluoride (HF) in H_2, HD, and D_2 complexes of varying size, up to and including the point where the first solvation shell is completed.[3] The sensitivity and resolution required for this study was achieved by using the pendular state method to collapse the rovibrational band contours into single narrow peaks.[7,8] Although this study did not provide rotational constants for these complexes, unique assignments (up to $n = 7$) were made possible by varying the ortho/para mixture of the hydrogen gas used in the pickup cell and by studying the pressure dependence of the various bands.[3] In this case, the HF was found to undergo free-rotation in HD complexes larger than $n = 8$. However, free rotation was not observed in the H_2 and D_2 complexes, owing to the much larger solvent anisotropy associated with the mixed ortho/para solvent shell.[3]

In the present study we present rotationally resolved spectra for the hydrogen-HF complexes in the range $n = 2$ to $n = 6$. Although the rotational constants obtained from these droplet experiments are modified from the gas phase values by the helium solvent, the corresponding spectra still provide detailed insights into the structure and dynamics of these complexes. In any case, the corresponding gas phase data is not presently available.

Experimental Section

The experimental approach used here has been discussed in several recent papers,[2,3,9] and further details on the design of the helium nanodroplet apparatus,[10] and the laser system,[11] can also be found elsewhere. Pure helium droplets were formed by free jet expansion from a cold nozzle. After passing through a skimmer, the droplets were doped with HF and hydrogen using the pick-up method. The source was operated at a typical stagnation pressure of 50 atm and a temperature of 20 K, resulting in the formation of helium droplets with an average size of 3700 atoms[12] and a radius of 3.5 nm.[13] The gas-phase samples were introduced into the pick-up cell via metering valves, and the pressures were fixed at the optimum pressures for formation of the clusters of interest ($\sim 1 \times 10^{-6}$ Torr for HF and $(1-3) \times 10^{-6}$ Torr for H_2), as described elsewhere.[2,3]

[†] Current address: FOM Institute for Plasma Physics "Rijnhuizen", Nieuwegein, The Netherlands.

10.1021/jp0310403 CCC: $27.50
Published on Web 02/21/2004

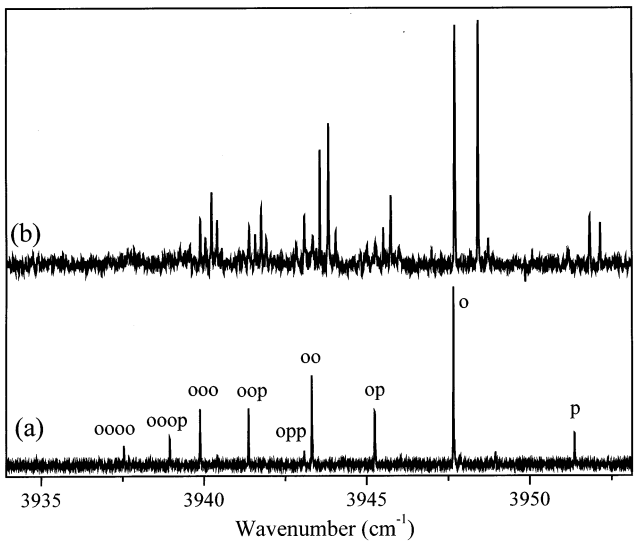

Figure 1. (a) Pendular and (b) field-free spectra of the $(H_2)_n$-HF complexes, recorded using similar droplet beam conditions and pickup cell pressures. The pendular peaks are labeled according to the ortho−para composition, using the notation described in the text.

Vibrational excitation of the clusters formed in the droplets was accomplished using a tunable F-center laser (Burleigh, crystal #2), which crosses the droplet beam many times in a multipass cell.[10] The vibrational energy in the complexes is then relaxed to the droplet, causing the evaporation of several hundred helium atoms. The corresponding decrease in the total energy of the droplet beam is detected using a cryogenically cooled bolometer (Infrared Laboratories). The laser is amplitude modulated and phase sensitive detection is used to obtain background free spectra.

The 3:1 (2:1) nuclear spin statistics of ortho and para H_2 (D_2) are reflected in molecular hydrogen even at the low helium droplet temperatures, due to slow spontaneous interconversion of the nuclear spins. For some of the spectra recorded here we made use of a home-built ortho/para hydrogen converter to enhance the signals associated with the para hydrogen complexes.[3] The earlier design was improved somewhat by enclosing the catalyst in a fritted glass ampule to minimize the contamination problems reported previously.[3]

Results

As mentioned above, we have previously reported pendular spectra for hydrogen-HF clusters of varying sizes and ortho/para compositions.[3] A survey scan comparing the pendular and field free spectra of $(H_2)_n$-HF clusters is shown in Figure 1, where rotationally resolved bands are clearly apparent up to $n = 3$. The two pendular peaks labeled o and p correspond to the binary ortho H_2-HF and para H_2-HF complexes, respectively, the rotationally resolved spectra of which have been discussed in detail previously.[9] The focus of the present paper will be on the larger complexes, labeled in Figure 1 according to the numbers of ortho and para hydrogens they contain.[3] It is useful to keep in mind that the different nuclear spin species of hydrogen have significantly different interactions with HF, owing to the electric quadrupole moment of hydrogen that persists in the $J = 1$ rotational species (ortho-H_2 and para-D_2) but is averaged to zero in $J = 0$ rotational species (para-H_2 and ortho-D_2). Note that these designations are only approximate for hydrogen molecules in the complexes, because the H_2-HF pair potential has fairly large anisotropic tems,[14,15] which will mix a small amount of $J = 2$ character into the rotational wave functions of the nominally $J = 0$ species. Nonetheless, it is still true that the quadrupole moment contributes much less to the interactions of the $J = 0$ rotational species with HF.[9,15−17]

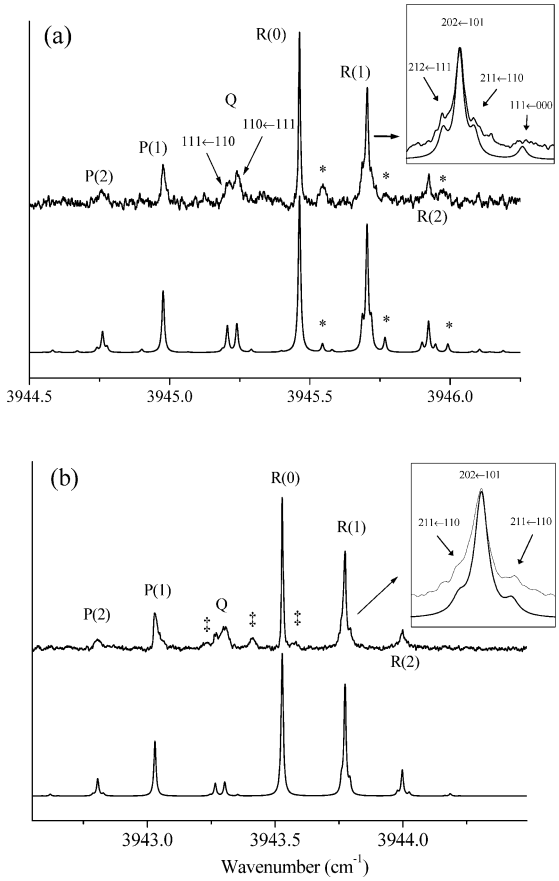

Figure 2. (a) Field free spectrum of the $(H_2)_2$-op-HF complex in helium droplets. Peaks marked with asterisks are assigned to a weakly allowed b-type band of the complex. The asymmetry splitting of the R(1) line is shown more clearly in the inset, along with the R(0) transition from the perpendicular b-type band (see text). (b) Field free spectrum of $(H_2)_2$-oo-HF in helium. The inset shows the asymmetry splitting of the R(1) line. The "‡" peaks are assigned to R-branch transitions of the $(H_2)_3$-opp-HF cluster (see text), whereas the blue shoulder on the P(1) peak is assigned to the corresponding Q-branch. The smooth curves in both panels are calculated spectra based on the fitted rovibrational constants (Table 1).

$(H_2)_2$-HF Complexes. Each of the vibrational bands shown in Figure 1 were recorded with higher sensitivity and using slower frequency scans for the purpose of obtaining accurate molecular constants. It is well-known that rotational fine structure in helium droplet spectra can be described using a gas-phase energy level expression[18] with modified constants to account for the effects of the helium. Figure 2a shows a high-resolution spectrum of the $(H_2)_2$-op-HF complex. A cursory inspection of this spectrum reveals that it is an A-type band of a near prolate asymmetric top. The spectrum is dominated by transitions originating from $K_a = 0$, as indicated in the figure using standard R and P branch notation. The Q branch, which shows clear asymmetry splitting, contains lines originating from $K_a = 1$; these are labeled according to the individual asymmetric top states (JK_aK_c notation) coupled by the transition. Asymmetry splitting is also evident in the R(1) line, as clearly seen in the inset. All of these results are consistent with a "T-shaped" complex, with the two hydrogens forming a dimer, to which the HF molecule is weakly bonded. In cases where the two H_2 molecules are of the same species (e.g., $(H_2)_2$-pp-HF), the complex is expected to have C_{2v} symmetry, as discussed below.

TABLE 1: Rotational Constants for $n = 2$ Clusters of HF with Different Combinations of the Spin Species of H_2 and D_2[a]

	H_2 complexes			D_2 complexes		
constant	para−para	ortho−para	ortho−ortho	ortho−ortho	ortho−para	para−para
A''	0.250 (10)	0.435 (10)	0.430 (10)	0.25 (2)	0.25 (2)	*d*
A'	0.255 (10)	0.438 (10)	0.436 (10)	0.25 (2)	0.25 (2)	*d*
B''	0.125 (2)[b]	0.129 (2)	0.134 (2)	0.131 (2)	0.125 (2)	0.109 (2)[b]
B'	0.128 (1)[b]	0.133 (1)	0.136 (1)	0.136 (1)	0.130 (1)	0.110 (2)[b]
C''	*b*	0.112 (2)	0.114 (2)	0.095 (2)	0.095 (2)	*b*
C'	*b*	0.117 (1)	0.119 (1)	0.094 (1)	0.095 (1)	*b*
D_J ($\times 10^{-4}$)[b]	6.0 (1)	6.0 (1)	5.8 (1)	10.0 (9)	8.0 (5)	6.4 (2)
ν_0	3947.748 (3)	3945.215 (3)	3943.275 (2)	3943.568 (2)	3942.061 (2)	3940.781 (1)
fwhm (MHz)	300	300	300	390	390	

[a] All constants are in cm^{-1} unless otherwise noted. Numbers in parentheses represent standard deviations in the last 1 or 2 digits (1σ). [b] The asymmetry splitting was not observable in the spectrum; thus the reported B constants represent the quantity $(B + C)/2$, determined from the $K_a = 0$ line positions (see text.) [c] D'' and D' were set equal in the fit (see text) [d] Could not be fit due to overlap with HF-$(D_2)_3$-ooo spectrum (see text).

The fit to the experimental spectrum was accomplished by first fitting the $\Delta K_a = 0$ transitions to a linear molecule energy level expression to determine $(B + C)/2$ for both the ground and excited vibrational states, as well the distortion constants (D_J) and the vibrational band origin (ν_0). The assumption that $D_J' = D_J''$ was made in this fit to keep the number of adjustable parameters consistent with the number of lines in the spectrum. The next step involved determining $B - C$ for both the ground and vibrationally excited states by fitting the asymmetry splittings in the Q branch and R(1) transition. The value of A'' was estimated from the relative intensities of the lines, whereas $(A'' - A')$ was determined from the position of the Q branch relative to the P and R branches. The constants obtained from this fit are summarized in Table 1.

In addition to the intense $\Delta K_a = 0$ transitions in the spectrum, there are a number of weaker peaks, labeled with asterisks in the figure. Using the rotational constants determined above, we were able to assign these as perpendicular (B-type) K_a: $1 \leftarrow 0$ transitions. Because this complex contains one ortho and one para hydrogen, it has C_s symmetry and the $\Delta K_a = \pm 1$ transitions are weakly allowed. The line intensities in the calculated spectrum in Figure 2a were obtained from a Boltzmann distribution at 0.37 K and a relative weighting of $\mu_B = 0.3\mu_A$ for the components of the transition dipole. The Lorentzian line width in the calculated spectrum is 300 MHz. Although the agreement between the positions of the calculated and experimental lines is excellent, the line widths and shapes show discrepancies that are quite typical of what is observed in helium droplets.[19−21] One particular feature of note in this case is that the line widths associated with parallel transitions coupling $K_a = 1$ states are somewhat broader than those coupling $K_a = 0$ states.

Figure 2b shows the spectrum of the $(H_2)_2$-oo-HF complex, which is quite similar to that of the $(H_2)_2$-op-HF complex. The same fitting procedure was used in this case, producing the constants given in Table 1, and the calculated spectrum shown in the figure. Once again, the agreement with experiment is excellent. The primary difference in the analysis of this spectrum comes from the fact that this complex has higher symmetry, namely C_{2v}, which requires that nuclear spin statistics be taken into account to properly reproduce the experimental line intensities. Given that the total spin of the ortho hydrogen is unity, the $(H_2)_2$-oo-HF complex has a 2:1 nuclear spin weight for the even and odd K_a states, respectively. Another consequence of the C_{2v} symmetry is that the B-type transitions are forbidden and are indeed absent from the spectrum. The peaks in the spectrum marked with a ‡ are assigned to the $(H_2)_3$-opp-HF cluster, which is expected to overlap this region, on the basis of the pendular spectroscopy[3] (see Figure 1).

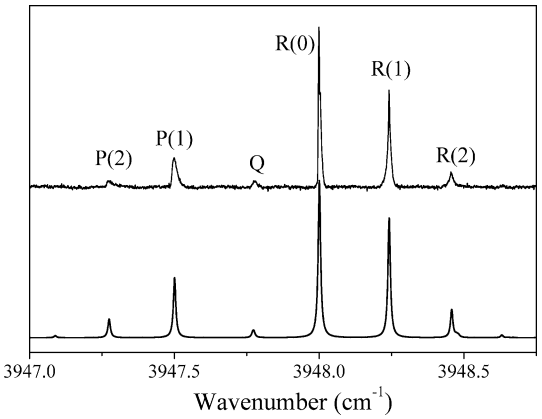

Figure 3. Field free spectrum of the $(H_2)_2$-pp-HF complex in helium, recorded using para-enriched H_2 (>98% para). The smooth curve was calculated using the fitted constants in Table 1.

The field free spectrum of $(H_2)_2$-pp-HF, shown in Figure 3 (fitted constants in Table 1), was obtained by using a para enriched hydrogen sample. The nuclear spin statistics resulting from the C_{2v} structure are clearly evident in the spectrum. Because para hydrogen is a spin zero boson, transitions arising from states with odd K_a are missing from the spectrum. This explains the dramatic reduction in the Q-branch intensity, because the lowest states that can contribute are $K_a = 2$ states, which have little population at 0.37 K. Unfortunately, because the K_a: $1 \leftarrow 1$ transitions were used above in the determination of the asymmetry splittings, we were unable to independently determine B and C constants for this cluster.

$(D_2)_2$-HF Complexes. Rotationally resolved spectra were also recorded for the ortho-ortho and ortho-para $(D_2)_2$-HF clusters, as shown in Figure 4a,b, respectively. Qualitatively, the spectra of these systems are rather similar to those of the ortho-ortho and ortho-para H_2 clusters, although with considerably larger asymmetry splittings. The assignment of the lines is exactly analogous to the corresponding $(H_2)_2$-HF complexes, except that the perpendicular band is not observed for the mixed ortho-para complex (see below). It is also interesting to note that a Q branch is observed in the ortho-ortho cluster, which for D_2 is a $J = 0$ rotational species. This is because the D atoms have a nuclear spin of unity, which in ortho-D_2 combine to give a total spin of 0 or 2 (para-D_2 is the spin 1 case). Because the degeneracy is $2S + 1$, the relative abundances of spin 0 and spin 2 oD_2 are 1:5. Of course, spin statistics will only be important for complexes where both of the oD_2 molecules have the same spin, because the rotational symmetry is broken in the mixed spin cases, making all K_a states allowed. When both oD_2's have spin 0 the situation is analogous to the pH_2 case,

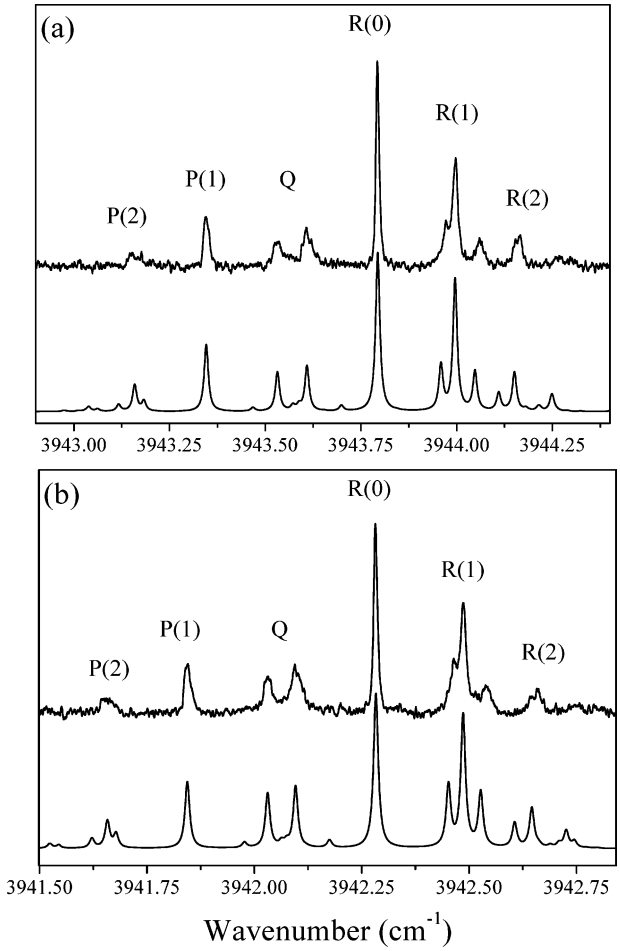

Figure 4. Field free spectra of the (a) $(D_2)_2$-oo-HF and (b) $(D_2)_2$-op-HF complexes in helium. The smooth curves were calculated using the fitted constants given in Table 1.

however, these have the lowest abundance (1 in 36). Complexes where both oD_2's are spin 2 have the highest abundance (25 in 36); the symmetry analysis of this case is straightforward and was carried out according to the procedure outlined by Bunker.[22] The end result is that the spin statistics for the $(D_2)_2$-oo-HF complex are 21:15 for the odd and even K_a states, as opposed to 0:1 in $(H_2)_2$-pp-HF.

As noted above, another important difference between these two systems is that the B-type transitions are not observed in the ortho-para D_2 cluster, although they are in principle allowed, because the complex has only C_s symmetry. This has important implications concerning the dynamics of the clusters, as discussed below. The constants obtained from fitting the above spectra are presented in Table 1 and the calculated spectra are shown in Figure 4. The quality of the fits is somewhat poorer than for the corresponding H_2 complexes. In particular, the positions of the $^{Q}R_1(1)$ transitions are not reproduced within the experimental uncertainty without including a large, negative value for D_{JK}, which has no clear physical interpretation.

The spectrum of the pp cluster is strongly overlapped by that of the ooo cluster (see Figure 6 below) and thus could not be accurately fit. However, there is no reason to expect the structure or spectrum to be particularly different than for the other $n = 2$ systems. Thus, estimated values of $(B + C)/2$ and ν_0 were obtained by fitting the $K_a = 0$ line positions to a linear rotor expression and are given in Table 1. Unfortunately, the Q-branch, which allowed independent determination of the A constant and $(B - C)$ values for the other $n = 2$ clusters, was

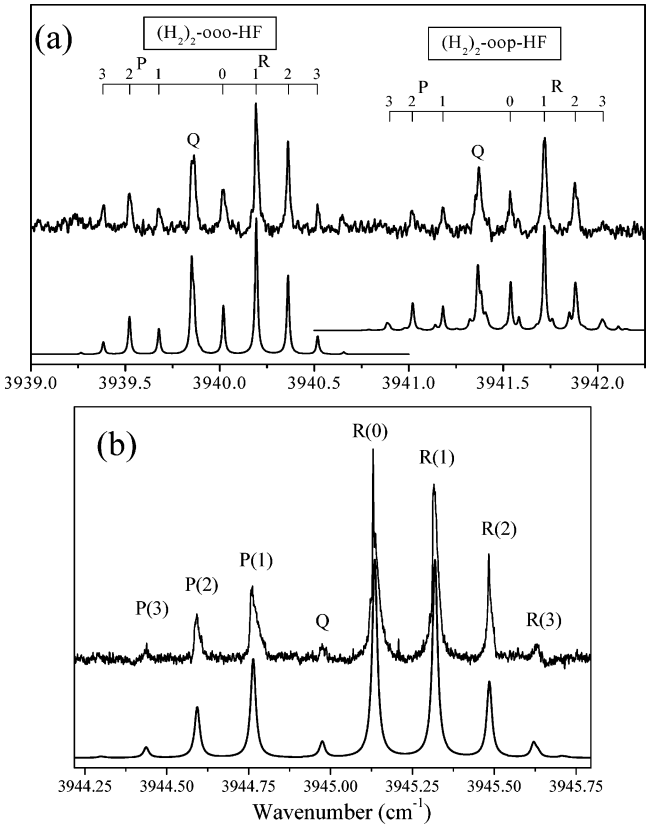

Figure 5. (a) Field free spectra of the $(H_2)_3$-ooo-HF and (b) $(H_2)_3$-oop-HF complexes in helium, the smooth curves having been calculated using the constants in Table 2 (see text). (b) Field free spectrum of the $(H_2)_3$-ppp-HF complexes in helium droplets, recorded using para-enriched H_2 (>98% para). The smooth curve was calculated using the fitted constants in Table 2.

obscured by the spectrum of the HF-$(D_2)_3$-ooo cluster, so those values could not be determined.

$(H_2)_3$-HF Complexes. Figure 5a shows a spectrum containing two bands assigned to $(H_2)_3$-ooo-HF and $(H_2)_3$-oop-HF, along with the calculated spectra as described below. The spectrum of the $(H_2)_3$-ooo-HF complex shows no evidence of asymmetry spitting and was fit to a prolate symmetric top Hamiltonian, using parallel selection rules; the fitted constants are collected in Table 2. This is consistent with a C_{3v} structure consisting of a trigonal planar hydrogen trimer to which the HF molecule is bound. Indeed, the relative intensities of the transitions in the $(H_2)_3$-ooo-HF complex could only be reproduced if the proper nuclear spin statistics were included (calculated according to the methods discussed by Bunker[22]).

The C_{3v} symmetry is broken in the oop cluster, which we found to be the cause of the irregular line shapes observed in the spectrum. In principle, this could be due to asymmetry splitting, although we found that it could not account for the perturbations in the experimental spectrum. Rather, the extra structure can be assigned to the perpendicular $K = 1 \leftarrow 0$ transitions. For example, the small peak just to the blue of the R(0) line is assigned to the perpendicular $1_1 \leftarrow 0_0$ transition. These B-type transitions were included in the calculated spectrum in Figure 5a, using the weighting $\mu_B = 0.35\mu_A$ for the components of the transition dipole, resulting in much improved agreement with the experimental spectra. We conclude that the effects of the symmetry breaking are weak enough so that the asymmetry splitting is within the experimental line width of 450 MHz ($B - C < 0.003$ cm^{-1}) but large enough to activate the perpendicular band of the complex. We will return to this

TABLE 2: Rotational Constants for $n = 3$ HF Clusters with Different Combinations of the Spin Species of H_2 and D_2[a]

	H_2 clusters			D_2 clusters		
constant	ooo	oop	ppp	opp	oop	ooo
A''	0.140 (10)	0.130 (3)	0.118 (10)	0.101 (1)	0.105 (1)	0.103 (1)
$(A'-A'')$	0.004 (1)	0.003 (1)	0.004 (1)	0.0025(10)	0.002 (1)	0.002 (1)
B''	0.0841 (2)	0.0891 (1)	0.0921 (5)	0.00743 (1)	0.0765 (1)	0.0771 (1)
B'	0.0873 (1)	0.0914 (1)	0.0957 (3)	0.00758 (1)	0.0778 (1)	0.0778 (1)
D'' ($\times 10^{-4}$)	2.4 (1)	4.2 (2)	2.8 (1)	1.6 (2)	3.6 (3)	2.8 (1)
D' ($\times 10^{-4}$)	2.4 (1)	3.8 (1)	3.9 (1)	2.3 (1)	3.3 (1)	2.8 (1)
ν_0	3939.845 (1)	3941.358 (1)	3944.948 (1)	3938.093 (1)	3939.234 (1)	3940.493 (1)
fwhm (MHz)	450	450	560	570	540	480

[a] All constants are in cm^{-1} unless otherwise noted. Numbers in parentheses represent standard deviations in the last 1 or 2 digits (1σ).

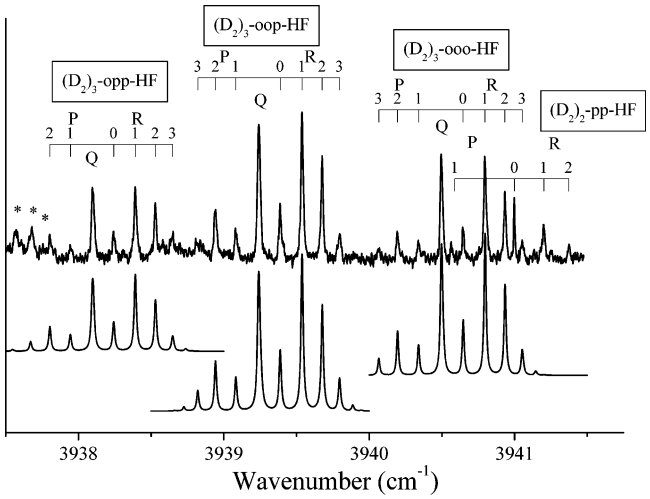

Figure 6. Field free spectra for various $(D_2)_3$-HF complexes. Note that the $(D_2)_2$-pp-HF spectrum overlaps the $(D_2)_3$-ooo-HF spectrum and that the unassigned features (marked with asterisks) to the red of the $(D_2)_3$-opp-HF spectrum arise from a complex containing four D_2 molecules. The smooth curves were calculated for the $(D_2)_3$-ooo-HF, $(D_2)_3$-oop-HF, and $(D_2)_3$-opp-HF clusters using the constants in Table 2 (see text).

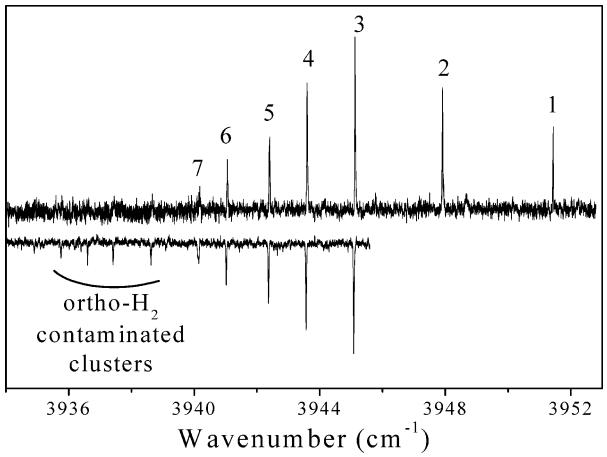

Figure 7. (a) Pendular spectra taken using para-enriched hydrogen, showing pure para $(H_2)_n$-HF clusters up to size $n = 7$. (b) Pendular spectra taken using larger droplets and a lower purity sample of para hydrogen; the peaks furthest to the red correspond to ortho-contaminated clusters (see text).

point further on in the discussion section. One final note is that, as mentioned above, the spectrum of the $(H_2)_3$-opp-HF cluster overlaps with that of $(H_2)_2$-oo-HF (see Figure 2b), preventing us from obtaining a quantitative fit to the data.

The spectrum of the $(H_2)_3$-ppp-HF cluster, recorded using para-enriched H_2, is shown in Figure 5b. This spectrum is qualitatively different than for the other $n = 3$ clusters, in that the Q-branch intensity is much weaker. This is once again due to the boson nuclear spin statistics associated with C_{3v} symmetry, which only allows population in states where K is an integer multiple of 3. As with $(H_2)_2$-pp-HF, the calculated intensities, and therefore the A rotational constants, were determined using this criterion. A fit to a symmetric top Hamiltonian yielded the constants given in Table 2 and the calculated spectrum shown in Figure 5b.

$(D_2)_3$-HF Complexes. Spectra for the corresponding D_2 $n = 3$ complexes were also recorded, as shown in Figure 6. Bands assigned to the ooo, oop, and opp clusters are shown in the figure, and although the opp spectrum overlaps with that of $(D_2)_4$-ooop-HF (assigned from the pendular data[3]), a sufficient number of transitions were assigned to obtain an accurate fit. Note also that there are some peaks present in the region of the ooo spectrum that are assigned to the $(D_2)_2$-pp-HF cluster (see above). Finally, the extra intensity between 3938.5 and 3939.0 cm^{-1} is due to the $(D_2)_4$-oooo-HF cluster, as assigned from the pendular data.[3]

As with the $n = 3$ H_2 clusters, the spectra were fit to symmetric tops, with the resulting constants collected in Table 2. Although, in principle, spin statistics are important for the pure oD_2 cluster, the broken symmetry cases (mixed spin 0 and spin 2) are most abundant and the spin statistics do not have a significant effect on the overall relative intensities. For this reason, the spectrum does not provide conclusive evidence for the C_{3v} symmetry of the pure ortho complex, as it did for the case of the analogous hydrogen complex.

Larger Complexes ($n > 3$). The improvements to our para-conversion apparatus (see Experimental Section above) allowed us to increase the purity of our para-enriched samples, beyond the level of 75% reported in our previous pendular study.[3] This can be seen from the pendular spectra in Figure 7. The upper trace was recorded first with a pickup pressure of 3×10^{-6} Torr of hydrogen from the improved converter. Pendular peaks for clusters up to $n = 7$ are clearly evident in the spectrum, with no sign of ortho contamination. The lower trace (shown inverted) was recorded with a lower purity sample of para-H_2, using larger droplets (20.0 K and 65 bar) and 5×10^{-6} Torr of hydrogen. Although the same peaks are observed here, additional peaks corresponding to ortho-H_2 contaminated clusters are seen further to the red. For the $(HD)_n$-HF clusters studied previously, no pendular peaks were observed for clusters larger than $n = 8$, which was taken as an indication that the HF began rotating freely in clusters with $n \geq 9$.[3] The spectra in Figure 7 tend to suggest that this occurs for $n \geq 8$ for para-H_2; however, the presence of the ortho-H_2 contaminated clusters complicates the picture somewhat. The difference between the $(HD)_n$-HF and $(H_2)_n$-HF could be the result of the larger zero point energy of the latter, which makes the corresponding clusters more "fluid", reducing slightly the number of solvent molecules needed to enable the HF to rotate. It is interesting to note that free-rotation

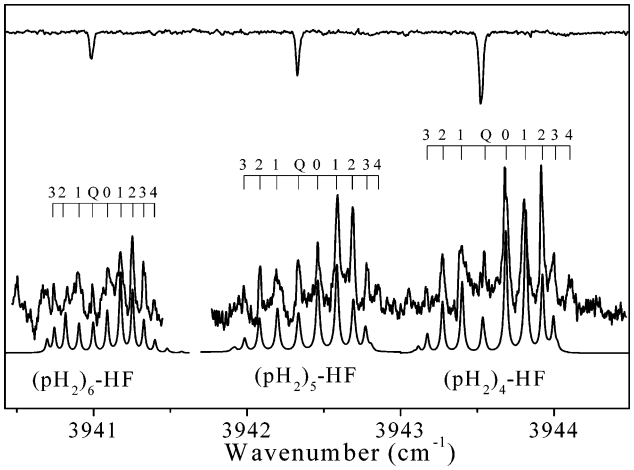

Figure 8. Rotationally resolved spectra of the pure para $(H_2)_4$-HF, $(H_2)_5$-HF, and $(H_2)_6$-HF complexes. The smooth spectra are the fits to the experimental data, with the corresponding molecular constants given in Table 3. The inverted pendular spectrum shown along the top of the figure shows the vibrational band origins.

TABLE 3: Fitted Constants (cm^{-1}) for the HF Doped Pure Para Hydrogen Clusters with $n = 4-6$[a]

	symm	$n = 4$	$n = 5$	$n = 6$
A	C_1	0.42	0.35	0.38
	C_{2v}	0.14	0.12	0.15
	C_{3v}	**0.073**[b]	**0.066**[b]	0.072
	C_{4v}	0.041	0.037	**0.049**[b]
B''		0.0703	0.0667	0.0470
B'		0.0697	0.0655	0.0459
$D_J'' \times 10^4$		3.50	4.75	2.82
$D_J' \times 10^4$		3.78	3.38	1.66
ν_0		3943.544	3942.336	3940.998

[a] Different values of A are given for the different possible symmetries for the clusters, taking into account the nuclear spin statistics (see text). [b] "Best-fit" values for A constants, according to the arguments presented in the text.

of light rotors is observed even in solid para-H_2, where HCl and DCl have been observed to undergo only slightly perturbed free rotation.[23] Thus even at the much higher density of solid pH_2, the overall potential is sufficiently isotropic to allow free rotation of HCl, and HF should behave similarly given that its rotational constant is a factor of ~2 (4) larger than for HCl (DCl).

Rotationally resolved spectra were obtained for $(pH_2)_n$-HF clusters for $n = 4-6$, as shown in Figure 8. These are all assigned as prolate symmetric tops, although there are some small discrepancies, as discussed below. The fitted rotational constants for these spectra are collected in Table 3, and corresponding calculated spectra are shown as smooth curves in Figure 8. The fitting of the A constants in these spectra required some additional care, because the symmetries of the corresponding clusters could not be reliably determined from the spectra. As a result, we were forced to estimate the A rotational constants on the basis of several different assumptions about the symmetries (C_1 through C_{4v}). Once again, the A rotational constant comes from fitting the Q-branch intensity (relative to that of the R and P branches) for each cluster. In our previous study of $(HD)_n$-HCN we found that the A and B rotational constants approached one another with increased numbers of solvent molecules, consistent with the complexes becoming more spherical as the first solvent shell begins to fill. On the bais of this, C_{3v} seems most reasonable for $n = 4$ and $n = 5$, whereas C_{4v} works best for $n = 6$. The structural ramifications of these symmetry determinations are discussed further below.

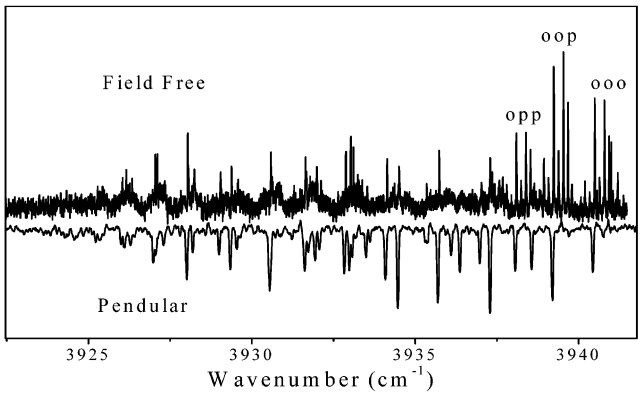

Figure 9. Comparison of the pendular and field-free spectra for $(D_2)_n$-HF complexes with $n > 3$.

Rotationally resolved spectra for the higher order complexes of H_2 and D_2 are not reported here for the mixed ortho/para species, due to the complexity of the spectra and the overlap between the bands. This is illustrated by the comparison between the pendular and field free spectra of larger D_2 clusters, shown in Figure 9. Note the correlation between what appear to be Q branches in the field free spectra and the pendular peaks in the lower spectrum.

It is worth noting that rotationally resolved spectra were not obtained for the corresponding $(HD)_n$-HF complexes (pendular spectra were obtained in our previous study[3]) owing to the substantial line broadening in these systems. This was noted in our previous study of the HD-HF binary complex, where the broadening was tentatively assigned to near-resonant vibrational energy transfer between the HF and the HD.[9]

Discussion

Smaller Complexes ($n = 2, 3$). Although rotational constants can often be used to quantitatively determine bond lengths in gas-phase molecules, the corresponding data for helium solvated molecules is complicated by the fact that the solvent contributes to the effective moments of inertia. Although considerable progress is being made in understanding these effects,[9,24,25] the theory is not sufficiently developed to permit the determination of accurate bond lengths. For the hydrogen clusters considered here, the situation is further complicated by the large zero point motion, which is likely to make vibrational averaging a significant issue. Nevertheless, the nuclear spin statistics and vibrational band types do provide information on the symmetry and overall structure of these systems. Furthermore, by comparing similar systems using isotopic substitution, meaningful information can be extracted from the rotational constants in helium, as has recently been shown for $(pH_2/oD_2)_n$-OCS complexes.[5]

We begin by considering clusters of the same n, which differ only in their ortho/para compositions. For example, consider the $n = 2$ H_2 clusters, which are nominally T-shaped, with the HF aligned along the A inertial axis. The most obvious difference between these systems is in the A rotational constant, which is almost a factor of 2 smaller for the pp complex, compared to that of oo or op. On the other hand, $(B + C)/2$ is only slightly larger for the pp cluster, compared to the other two. The implication is that the vibrationally averaged pp complex has a larger hydrogen−hydrogen distance than the other two, which makes sense, given that para-H_2 has essentially no quadrupole moment, making its interactions with both HF

and the other H_2 molecule weaker than for ortho hydrogen.[15,16] An increased hydrogen−hydrogen distance will clearly result in a smaller *A* value, the effect likely being amplified by the corresponding increase in the amount of helium that has to move to accommodate the motion of the complex. The reason behind the increase in $(B + C)/2$ is less clear, although it is consistent with the HF undergoing wider amplitude vibrational motion, allowing it to move slightly closer to the center-of-mass of the two hydrogens.

We now consider the effects of symmetry breaking in the op cluster. Because the HF interacts more strongly with the ortho hydrogen than with para, we expect that the vibrationally averaged orientation of the HF bond axis will no longer be along the *A* inertial axis of the complex, as it is in the oo and pp cases. From the relative intensities of the *A*-type and *B*-type bands in the above spectrum of the op complex, we can estimate that the vibrationally averaged angle of the HF bond with the *A* axis is ∼17°. It is interesting to point out that our previous study of the pendular spectroscopy of these complexes[3] gave independent confirmation of these effects. In particular, we found that the vibrational shifts associated with adding para hydrogen to complexes of a given size decreased with increasing ortho hydrogen content, the implication being that the ortho hydrogens dominated the interactions with the HF molecule.[3]

For the $n = 2$ D_2 complexes the most weakly bound oo complex ($J = 0$ species) has essentially the same rotational constants as the op complex. The implication is that the lower zero point energy associated with the D_2 clusters reduces the effects described for the $n = 2$ H_2 complexes above. Another contributing factor may be that the lower rotational constant of D_2 (∼30 cm^{-1}) compared with H_2 (∼60 cm^{-1}) allows more mixing of the $J = 2$ and $J = 0$ states due to the anisotropy of the pair potential (as discussed above) than for para-H_2. This would increase the contribution of the electrostatic dipole−quadrupole and quadrupole-quadrupole terms to the oD_2-HF interaction, making it more similar to pD_2-HF. Both of these effects are consistent with the fact that the B-type transitions are not observed in the mixed ortho-para D_2 cluster, suggesting that the HF is more equally shared between the ortho and para species, compared to what is seen for H_2. Once again, similar conclusions were reached on the basis of the data in the pendular spectroscopy study reported previously.[3]

The trends observed in the rotational constants of the $n = 3$ clusters (Table 2) are essentially the same as those above for $n = 2$. Indeed, for the H_2 complexes the *A* constant decreases as the composition goes from pure ortho- to pure para-H_2, whereas the *B* constants are seen to increase. Once again, this suggests that the pH_2 molecules are more delocalized than the oH_2. In addition, the complex with broken symmetry (oop cluster) shows perpendicular transitions, again reflecting the stronger interaction with the ortho-H_2. In this case the vibrationally averaged structure has the HF deflected away from the *A* axis by ∼19°, with the angular probability distribution for the HF peaked in the direction of the two oH_2 molecules. Finally, the three $n = 3$ D_2 clusters have very similar rotational constants and perpendicular bands are not observed when the symmetry is broken in the oop and opp complexes. This is again consistent with the picture that the lower zero point energy makes the ortho-D_2 and para-D_2 interactions more equivalent.

So far we have not said anything about the differences in the rotational constants between the ground and excited vibrational states. The primary point of interest here is that for $n = 2$ and $n = 3$, all of the rotational constants are larger in the excited states. This makes sense given that vibrational excitation increases the dipole moment of the HF, thereby strengthening the HF−H_2 intermolecular interactions, which in turn causes a general contraction of the corresponding bond lengths.

We now comment on a few of the peculiarities in the spectra that were noted above. To begin with, consider the fact that *negative* D_{JK} constants were required for an accurate fit of the spectra of the $(D_2)_2$-HF complexes. In general, distortion constants for spectra taken in liquid helium droplets are consistently found to be several orders of magnitude larger than in the gas phase. The exact mechanism for this is not yet known, although it is generally thought to result from the response of the helium to molecular rotation.[26] Because there is independent evidence from the line widths that different K_a states can interact differently with the helium, this may also be the reason for the negative D_{JK} constant, although the particular mechanism is not at all clear. Finally, we note that the line widths observed for the D_2 complexes are larger than for the H_2 complexes, in both the $n = 2$ and $n = 3$ cases. This was also observed for the binary complexes in helium droplets,[9] and also in the gas phase,[17,27] where it was attributed to intermolecular vibrational energy transfer. A similar mechanism may be responsible for the line widths in these larger clusters.

$(pH_2)_n$-HF Complexes ($n = 4-6$). We now turn to the larger clusters of pure para hydrogen with HF. In their study of the $(pH_2)_n$-OCS clusters, Grebenev et al. were able to deduce structural information using symmetry arguments, on the basis of trends in the relative intensity of the Q branches in the spectra, as a function of cluster size. For example, Q branches were not observed in the spectra for the $n = 5$ and $n = 6$ clusters, and this was taken as evidence of high symmetry structures, namely rings or bolts of pH_2 molecules around the OCS.[5]

What can we say here about the structures of the para $(H_2)_n$-HF ($n > 3$) complexes? The $n = 4$ cluster appears the easiest to understand a priori, because the pH_2 molecules can form a capped trigonal planar arrangement over the HF, which would be consistent with the observed C_{3v} symmetry. On the other hand, the large incremental red shift going from $n = 3$ to $n = 4$ also indicates that the pH_2 is solvating the HF,[3] and studies on analogous solvated systems such as Ar_4-HF indicate that an "opened" C_{2v} symmetric structure is preferred in this case.[28,29] Of course there is considerably more zero-point energy in the pH_2 clusters, so it may be that this allows the C_{3v} structure to be maintained, while still allowing the capping pH_2 to approach close enough to produce the observed redshift. At this point we can say little more about the structure of this complex.

The $n = 5$ and $n = 6$ para hydrogen clusters are even more problematic. For instance, a solvated structure for the 5 pH_2 complex should not have C_{3v} symmetry if the complex is rigid. A similar problem exists for the $n = 6$ case, where the suggested symmetry is C_{4v}. Once again the large zero-point energies provide a potential explanation for this. For purposes of illustration, imagine an extreme case where the pH_2 molecules are completely delocalized in the first solvent shell, basically forming a cloud around the H-end of the HF molecule. In this case, the system would effectively have cylindrical symmetry, and the A-rotational constant and apparent symmetry, as determined by the indirect methods used here, would depend on the average arrangement of the pH_2 molecules in the cloud. This picture is quite similar to what was concluded for the analogous $(HD)_n$-HCN clusters, where symmetric top spectra were also observed for clusters with incomplete solvent shells.[2] Unfortunately, we cannot draw definite conclusions based on the data presented here, but the close analogy with the $(HD)_n$-HCN systems gives some support for this picture of delocalized

hydrogen molecules. Quantum mechanical calculations, like those of Kwon and Whaley,[4] using Path Integral Monte Carlo (PIMC) methods, could provide further insights into these systems.

One final point concerns the aforementioned discrepancies in the symmetric top fits to the observed spectra of the $n = 4-6$ $(pH_2)_n$-HF complexes. In each spectra there is at least one feature that is not reproduced by the calculations: there are peaks at the blue extrema of the $n = 4$ and $n = 5$ complexes, and there seems to be an intense feature "underneath" the P-branch of the $n = 6$ spectrum. In the particular case of $n = 4$, if the R(2) line is assumed to be perturbed, then the fit can be modified to include the two peaks furthest to the blue. However, then the fitted D-constants become so large that unphysical effects appear elsewhere in the spectrum (e.g., the $J = 5$, $K = 0$ state has a negative energy). The origin of these unreproduced features is not apparent at this time. One possible explanation is that the extreme floppiness of the system causes a shifting of the energy levels that cannot be reproduced with a rigid rotor model.[30] Another possibility is that the interactions with the helium droplet are perturbing the rotational levels. Once again, a conclusive determination must await high-level computational results.

Conclusions

Rotationally resolved spectra have been reported for a wide range of (hydrogen)$_n$-HF complexes. In general, the smaller ($n = 2$, 3) clusters have prolate or near-prolate top structures, namely, T-shaped (C_{2v}) for the $n = 2$ complexes and prolate symmetric top (C_{3v}) for the $n = 3$ complexes. The observation of perpendicular transitions in the H_2 complexes with mixed ortho/para composition supports a picture in which the HF molecule prefers to "point" in the direction of the ortho-H_2 molecules, because the interaction with ortho-H_2 is stronger. In these cases, the vibrationally averaged HF bond directions are significantly off the inertial axis, such that the resulting spectra are a hybrid A/B. Similar behavior is not observed for the mixed ortho/para D_2 clusters because the relative interactions of the ortho and para D_2 molecules with HF are much more similar,[15] primarily due to zero point energy effects. Field-free spectra for larger clusters ($n = 4-6$) of pure para hydrogen with HF were also reported and tentatively indicate that the structures of these clusters are also highly symmetric. This is most likely to a large degree of delocalization of the pH_2 molecules in the first solvent shell, due to their large zero-point energies.

Acknowledgment. Support for this research from the National Science Foundation (CHE-99-87740) and the Air Force Office of Scientific Research (AFOSR) is gratefully acknowledged.

References and Notes

(1) Grebenev, S.; Sartakov, B.; Toennies, J. P.; Vilesov, A. F. *Science* **2000**, *280*, 1532.
(2) Moore, D. T.; Miller, R. E. *J. Chem. Phys.* **2003**, *119*, 4713.
(3) Moore, D. T.; Miller, R. E. *J. Phys. Chem.*, In Press.
(4) Kwon, Y.; Whaley, K. B. *Phys. Rev. Lett.* **2003**, *89*, 273401−1.
(5) Grebenev, S.; Sartakov, B.; Toennies, J. P.; Vilesov, A. F. *Phys. Rev. Lett.* **2003**, *89*, 225301−1.
(6) Sindzingre, P.; Ceperley, D. M.; Klein, M. L. *Phys. Rev. Lett.* **1991**, *67*, 1871.
(7) Block, P. A.; Bohac, E. J.; Miller, R. E. *Phys. Rev. Lett.* **1992**, *68*, 1303.
(8) Rost, J. M.; Griffin, J. C.; Friedrich, B.; Herschbach, D. R. *Phys. Rev. Lett.* **1992**, *68*, 1299.
(9) Moore, D. T.; Miller, R. E. *J. Chem. Phys.* **2003**, *118*, 9629.
(10) Nauta, K.; Miller, R. E. *J. Chem. Phys.* **1999**, *111*, 3426.
(11) Huang, Z. S.; Jucks, K. W.; Miller, R. E. *J. Chem. Phys.* **1986**, *85*, 3338.
(12) Knuth, E. L.; Schilling, B.; Toennies, J. P. *Int. Symp. Rarefied Gas Dynamics, 19th* **1995**, 270−6.
(13) Lewerenz, M.; Schilling, B.; Toennies, J. P. *Chem. Phys. Lett.* **1993**, *206*, 381.
(14) Krause, P. J.; Clary, D. C. *Mol. Phys.* **1998**, *93*, 619.
(15) Clary, D. C.; Knowles, P. J. *J. Chem. Phys.* **1990**, *93*, 6334.
(16) Lovejoy, C. M.; Nelson, D. D., Jr.; Nesbitt, D. J. *J. Chem. Phys.* **1987**, *87*, 5621.
(17) Lovejoy, C. M.; Nelson, D. D., Jr.; Nesbitt, D. J. *J. Chem. Phys.* **1988**, *89*, 7180.
(18) Hartmann, M.; Miller, R. E.; Toennies, J. P.; Vilesov, A. F. *Phys. Rev. Lett.* **1995**, *75*, 1566.
(19) Nauta, K.; Miller, R. E. *Phys. Rev. Lett.* **1999**, *82*, 4480.
(20) Callegari, C.; Reinhard, I.; Lehmann, K. K.; Scoles, G.; Nauta, K.; Miller, R. E. *J. Chem. Phys.* **2000**, *113*, 4636.
(21) Grebenev, S.; Havenith, M.; Madeja, F.; Toennies, J. P.; Vilesov, A. F. *J. Chem. Phys.* **2000**, *113*, 9060.
(22) Bunker, P. R. *Molecular Symmetry and Spectroscopy*; Academic Press: New York, 1979.
(23) Anderson, D. T.; Hinde, R. J.; Tam, S.; Fajardo, M. E. *J. Chem. Phys.* **2002**, *116*, 594.
(24) Grebenev, S.; Sartakov, B.; Toennies, J. P.; Vilesov, A. F. *J. Chem. Phys.* **2001**, *114*, 617.
(25) Moore, D. T.; Ishiguro, M.; Miller, R. E. *J. Chem. Phys.* **2001**, *115*, 5144.
(26) Lehmann, K. K. *J. Chem. Phys.* **2001**, *114*, 4643.
(27) Bohac, E. J.; Miller, R. E. *J. Chem. Phys.* **1993**, *98*, 2604.
(28) Nauta, K.; Miller, R. E. *J. Chem. Phys.* **2001**, *115*, 10138.
(29) Liu, S.; Bacic, Z.; Moskowitz, J. W.; Schmidt, K. E. *J. Chem. Phys.* **1994**, *100*, 7166.
(30) Nesbitt, D. J.; Naaman, R. *J. Chem. Phys.* **1989**, *91*, 3801.